Acta Mech 228, 4039–4053 (2017)
DOI 10.1007/s00707-017-1941-1

ORIGINAL PAPER

Zai-lin Yang · Guan-xi-xi Jiang · Bai-tao Sun · Yong Yang

Scattering of shear waves by a cylindrical inclusion in an anisotropic half space

Received: 18 May 2017 / Revised: 3 July 2017 / Published online: 28 July 2017

Abstract Based on the complex function method and a multipolar coordinate system, scattering of shear waves by a cylindrical inclusion in an anisotropic (orthotropic) half space is studied. In order to find the solution of shear waves, the governing equation is transferred into its normalized form. Then, the scattering wave in the half space and the standing wave in the inclusion are deduced. Different incident wave angles and anisotropies are considered to obtain the reflected wave. Then, the unknown coefficients in scattering wave and standing wave are found by utilizing the continuous condition at the boundary of the inclusion. Subsequently, the dynamic stress concentration factor (DSCF) around the inclusion is calculated and analyzed. The results demonstrate that the distribution of the DSCF is influenced by the anisotropy of the half space, and the value of the DSCF is mainly affected by the wave numbers ratio and the shear modulus ratio.

1 Introduction

Dynamic stress analysis of elastic waves in a continuous medium or in continuous structures is significant for practical engineering. Besides, wave propagation in different kinds of medium also attracts a lot of attention in elastodynamics. Because different media and defects (cavities, inclusions or cracks) may influence the stresses in continuous media or structures, the dynamic response of elastic waves in the complex medium or medium with defects should be considered in materials science, structural damage detection, earthquake engineering, and many other fields.

Problems of elastic waves in media and structures have been discussed for centuries. Wave propagation in simple media firstly which attracted scholars' attention. Pao and Mow [1] researched diffraction of elastic waves in 1973. Moreover, dynamic stress concentration under different kinds of waves was also investigated by them. Wave propagation in elastic solids was expounded by Achenbach [2] in the same year. Liu et al. [3] studied dynamic stress concentrations around defects by the complex function method. The problem of

Z. Yang · G. Jiang · Y. Yang (✉)
College of Aerospace and Civil Engineering, Harbin Engineering University, Harbin, China
E-mail: yangyongheu@163.com

Z. Yang
E-mail: yangzailin00@163.com

G. Jiang
E-mail: jiang_910616@163.com

B. Sun
China Key Laboratory of Earthquake Engineering and Engineering Vibration, Institute of Engineering Mechanics, China Earthquake Administration, Harbin, China
E-mail: sunbt@iem.cn

plane SH wave scattering by a semicylindrical canyon was researched by Trifunac [4], and then, displacement amplitudes of different incident wave angles were analyzed. Subsequently, the surface displacement problem of a semi-elliptical canyon under SH waves was discussed by Wong and Trifunac [5]. Nowadays, wave motion problems in homogeneous and isotropic media are also popular in elastodynamics. Parvanova et al. [6] studied the dynamic response of a finite-size elastic plate containing multiple defects by using BEM. The model was subjected to time-harmonic loads along its perimeter, and anti-plane strain conditions were assumed. The same method was utilized to discuss the dynamic stress concentration for multiple multilayered inclusions embedded in an elastic half space by Sheikhhassani and Dravinski [7]. Xu et al. [8] investigated the dynamic response of complex defects near bimaterials' interface by incident out-plane waves. By utilizing complex function method and Green's function, the dynamic stress concentration factor around the cavity and the dynamic stress intensity factor at the crack were calculated and discussed. The axisymmetric time-harmonic response of a half space was studied by Eskandari et al. [9]. The half space is transversely isotropic and surface stiffened. The half space is reinforced by a Kirchhoff thin plate on its surface. Then, effects of anisotropy, depth of loading, bonding assumption, and frequency of excitation are discussed.

Except problems of wave propagation in simple media, wave motion problems in complex media, are hot as well. Liu and Han [10] researched scattering of SH waves by a noncircular cavity in anisotropic media. Based on complex function method, the dynamic stress concentration of rectangular and elliptical cavities was analyzed. Two formulations for the dynamic response of a cylindrical cavity in cross-anisotropic porous media were researched by Eslami and Gatmiri [11]. Then, pore pressure, radial stress, hoop stress, and shear stress at different points are obtained. C.H. Daros [12] investigated the Green's function for SH waves in an inhomogeneous anisotropic elastic solid. The wave velocity has a expression of power function, and the Green's function was derived to model transient SH waves. Then, the form of the wave front was given. Multiple scattering of elastic waves in heterogeneous anisotropic media was modeled by Baydoun et al. [13]. Relying on the kinetic approach, the waves are described in terms of their associated energy densities. The model has practical application meaning to metallic and mineral crystals. Similarly, wave propagation in elastic quasicrystals was researched by Wang and Schiavone [14]. The surface waves and interfacial waves were considered, and the quasicrystals were anisotropic. Then, the Stroh formalism was presented. Problems of SH waves propagating in anisotropic laminated plates were studied by Maigre and Kuznetsov [15]. A mathematical model was obtained to analyze propagation ability and the specific energy of SH waves. Different boundary conditions were considered, and then analytical solutions are presented. Scattering by an anisotropic circle was researched by Bostrm [16]. The outside medium is isotropic, and the inside medium is orthotropic. The equation inside the circle is transformed to polar coordinates, and the far-field amplitude is obtained. The solution demonstrated that the anisotropy has strong effects on the scattering when the frequencies are high. A general ultrasonic scattering model for a polycrystal was obtained by Li and Rokhlin [17]. Numerical examples were given, and the scattering coefficients were obtained. An numerical analysis of an SH wave field was performed by Lee et al. [18]. By applying parallel volume integral equation method (PVIEM), wave scattering in an unbounded isotropic solid was analyzed. The numerical method is widely applicable for many kinds of elastodynamic problems.

This paper aims to research wave scattering by a cylindrical inclusion in an anisotropic (orthotropic) half space. A transformation is introduced in order to normalize the governing equation. Considering the anisotropy of the half space, the reflected wave is obtained. According to the image principle, the scattering wave in the anisotropic half space is derived. Then, the expression of stress components is given, and the unknown coefficients are solved using the boundary condition. Subsequently, dynamic stress concentration factors with different parameters are calculated and discussed.

2 Model description and basic equations

The scattering model of a cylindrical inclusion buried in a half space is described in Fig. 1. The half space (medium I) is homogeneous but anisotropic, while the homogeneous inclusion (medium II) is isotropic. The shear modulus and the mass density of medium I are μ_1 and ρ_1. Similarly, the shear modulus and the mass density of medium II are μ_2 and ρ_2. The origin of the polar coordinate system coincides with the center of the inclusion. The radius of the inclusion is R, and the buried depth of the inclusion is h. The incident angle of shear waves is a_i, and the reflected angle is a_r. Because the medium of the half space is anisotropic, the reflected angle does not equal the incident angle. The surface of the half space is at $y_1 = 0$. The conversion

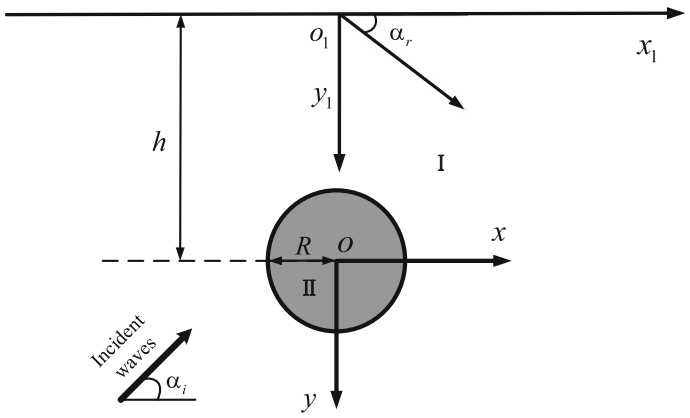

Fig. 1 Model of the problem

relation between xoy and $x_1o_1y_1$ can be expressed as

$$x_1 = x,\ y_1 = y - h. \tag{1}$$

Under the shear model for the problem, the anisotropic parameters corresponding to the shear parts need to be considered only. Hence, the anisotropic problem degenerates to an orthotropic one, and only three anisotropic parameters (c_{44}, c_{45} and c_{55}) are useful. In this condition, the governing equation in Cartesian coordinates (x, y) can be written as

$$c_{55}\frac{\partial^2\phi}{\partial x^2} + 2c_{45}\frac{\partial^2\phi}{\partial x\partial y} + c_{44}\frac{\partial^2\phi}{\partial y^2} = \rho\frac{\partial^2\phi}{\partial t^2}. \tag{2}$$

Introducing complex variables $z = x + iy$ and $\bar{z} = x - iy$, the governing equation in the complex plane $(z, \bar{z})$ has the form of

$$(c_{55} - c_{44} + 2ic_{45})\frac{\partial^2\phi}{\partial z^2} + 2(c_{55} + c_{44})\frac{\partial^2\phi}{\partial z\partial\bar{z}} + (c_{55} - c_{44} - 2ic_{45})\frac{\partial^2\phi}{\partial\bar{z}^2} = \rho\frac{\partial^2\phi}{\partial t^2} \tag{3}$$

where ϕ is the displacement function and ρ is the mass density of the anisotropic medium. c_{44}, c_{45}, and c_{55} are elastic constants which are independent of each other. The elastic constants take the following form:

$$c_{55} > 0,\ \left(c_{44}c_{55} - c_{45}^2\right) > 0. \tag{4}$$

A transformation is applied in order to normalize the governing equation,

$$\left.\begin{aligned}\chi &= \frac{1}{2}\left[(1 - i\gamma)z + (1 + i\gamma)\bar{z}\right]\\ \bar{\chi} &= \frac{1}{2}\left[(1 - i\bar{\gamma})z + (1 + i\bar{\gamma})\bar{z}\right]\end{aligned}\right\}, \tag{5}$$

where $\gamma = -\dfrac{c_{45}}{c_{44}} + i\dfrac{\left(c_{44}c_{55} - c_{45}^2\right)^{\frac{1}{2}}}{c_{44}}$, $i = \sqrt{-1}$.

Substituting Eq. (5) into (3), the governing equation obeys

$$\frac{\partial^2\phi}{\partial\chi\partial\bar{\chi}} = \left[\frac{ik_T}{2}\right]^2\phi \tag{6}$$

where $k_T = \omega/c_T$ is the wave number, $c_T = \sqrt{\mu_1/\rho_1}$, $\mu_1 = \left(c_{44}c_{55} - c_{45}^2\right)/c_{44}$ is the shear modulus of the half space, ρ_1 is the mass density of the half space; ω is the circular frequency.

3 Wave fields and stress components

3.1 Expressions of wave fields

Suppose the plane shear wave propagates with the arbitrary angle a_i in medium I, the incident wave can be expressed as

$$\phi^{(i)} = \phi_0 \exp\left(\frac{ik_i}{2}\left[(z+ih)\,\beta_i + (\bar{z}-ih)\,\overline{\beta_i}\right]\right) \tag{7}$$

where ϕ_0 is the amplitude of the incident wave, $\beta_i = e^{i\alpha_i}$, $\bar{\beta}_i = e^{-i\alpha_i}$. $k_i = \omega/c_i$ is the wave number of the incident wave. c_i is the velocity with the direction of the incident wave which can be written as

$$c_i = \left[\frac{1}{\rho}\left(c_{55}\cos^2\alpha_i - 2c_{45}\cos\alpha_i \sin\alpha_i + c_{44}\sin^2\alpha_i\right)\right]^{\frac{1}{2}}. \tag{8}$$

Subsequently, with the aid of the stress-free condition at the surface, the reflected wave has the form of [19]

$$\phi^{(r)} = \phi_0 \exp\left(\frac{ik_r}{2}\left[(z+ih)\,\beta_r + (\bar{z}-ih)\,\overline{\beta_r}\right]\right) \tag{9}$$

where $k_r = \omega/c_r$ is the wave number of the reflected wave, c_r is the velocity of the reflected wave.

In an anisotropic half space, the expression of reflected wave velocity is determined by the incident angle α_i; if $\tan\alpha_i \geq 2c_{45}/c_{44}$, there is $\beta_r = e^{-i\alpha_r}$, $\bar{\beta}_r = e^{i\alpha_r}$, then $\tan\alpha_r = (\tan\alpha_i - 2c_{45}/c_{55})$. In this condition, c_r can be formulated as

$$c_r = \left[\frac{1}{\rho}\left(c_{55}\cos^2\alpha_r + 2c_{45}\cos\alpha_r \sin\alpha_r + c_{44}\sin^2\alpha_r\right)\right]^{\frac{1}{2}}. \tag{10}$$

If $\tan\alpha_i < 2c_{45}/c_{44}$, we have $\beta_r = e^{i\alpha_r}$, $\bar{\beta}_r = e^{-i\alpha_r}$, then $\tan\alpha_r = -(\tan\alpha_i - 2c_{45}/c_{44})$. Therefore, c_r has the following expression:

$$c_r = \left[\frac{1}{\rho}\left(c_{55}\cos^2\alpha_r - 2c_{45}\cos\alpha_r \sin\alpha_r + c_{44}\sin^2\alpha_r\right)\right]^{\frac{1}{2}}. \tag{11}$$

The scattering wave excited by the inclusion is

$$\phi^{(s)} = \sum_{n=-\infty}^{\infty} A_n \left\{H_n^{(1)}\left(k_T\,|\chi|\right)\left(\frac{\chi}{|\chi|}\right)^n + H_n^{(1)}\left(k_T\,|\chi_1|\right)\left(\frac{\chi_1}{|\chi_1|}\right)^{-n}\right\} \tag{12}$$

where A_n is a series of unknown coefficients, $H_n^{(1)}(\cdot)$ is the first kind Hankel function of the nth order, $\chi_1 = \frac{1}{2}\left[(1-i\gamma)\cdot(z+2hi) + (1+i\gamma)\,(\bar{z}-2hi)\right]$. The scattering wave can satisfy the stress-free condition at the surface and the Sommerfeld radiation condition at infinity automatically. The entire wave fields in medium I are the superposition of the incident wave, the reflected wave, and the scattering wave, which can be written as

$$\phi_I = \phi^{(i)} + \phi^{(r)} + \phi^{(s)}. \tag{13}$$

Because the homogeneous isotropic inclusion exists, the standing wave in medium II is

$$\phi^{(t)} = \sum_{n=-\infty}^{\infty} B_n J_n\left(k_2\,|z|\right)\left(\frac{z}{|z|}\right)^n \tag{14}$$

where B_n is another series of unknown coefficients.

Therefore, the entire wave fields in medium II are the standing wave

$$\phi_{II} = \phi^{(t)}. \tag{15}$$

3.2 Stress components

The stress components in Cartesian coordinate (x, y) in an isotropic medium are

$$\tau_{xz} = \mu \frac{\partial \phi}{\partial x}, \ \tau_{yz} = \mu \frac{\partial \phi}{\partial y}. \tag{16}$$

Hence, in cylindrical coordinate systems (r, θ, z), the stress components corresponding to the wave fields can be written as

$$\tau_{rz} = \mu \frac{\partial \phi}{\partial r}, \ \tau_{\theta z} = \mu \frac{1}{r} \frac{\partial \phi}{\partial \theta}. \tag{17}$$

In complex coordinate systems $(z, \bar{z})$, the constitutive equations of an isotropic medium become

$$\tau_{rz} = \mu \left(\frac{\partial \phi}{\partial z} e^{i\theta} + \frac{\partial \phi}{\partial \bar{z}} e^{-i\theta} \right), \tag{18}$$

$$\tau_{\theta z} = i\mu \left(\frac{\partial \phi}{\partial z} e^{i\theta} - \frac{\partial \phi}{\partial \bar{z}} e^{-i\theta} \right). \tag{19}$$

According to Hooke's law, the constitutive relations in an anisotropic medium between stress components and the wave fields obey

$$\begin{aligned} \tau_{rz} = & \frac{1}{2} \left[(c_{55} + c_{44}) \frac{\partial \phi}{\partial z} + (c_{55} - c_{44} - 2ic_{45}) \frac{\partial \phi}{\partial \bar{z}} \right] e^{i\theta} \\ & + \frac{1}{2} \left[(c_{55} - c_{44} + 2ic_{45}) \frac{\partial \phi}{\partial z} + (c_{55} + c_{44}) \frac{\partial \phi}{\partial \bar{z}} \right] e^{-i\theta}, \end{aligned} \tag{20}$$

$$\begin{aligned} \tau_{\theta z} = & \frac{1}{2} \left[i \left(c_{44} + c_{55} \right) \frac{\partial \phi}{\partial z} + \left(2c_{45} + i(c_{55} - c_{44}) \right) \frac{\partial \phi}{\partial \bar{z}} \right] e^{i\theta} \\ & + \frac{1}{2} \left[(2c_{45} + i(c_{44} - c_{55})) \frac{\partial \phi}{\partial z} - i \left(c_{44} + c_{55} \right) \frac{\partial \phi}{\partial \bar{z}} \right] e^{-i\theta}. \end{aligned} \tag{21}$$

In the coordinate systems $(\chi, \bar{\chi})$, Eqs. (20) and (21) can be shown to be

$$\begin{aligned} \tau_{rz} = & \frac{1}{4} \left\{ \left[(c_{55} + c_{44}) (1 - i\gamma) + (c_{55} - c_{44} - 2ic_{45}) (1 + i\gamma) \right] \frac{\partial \phi}{\partial \chi} \right. \\ & \left. + \left[(c_{55} + c_{44}) (1 - i\bar{\gamma}) + (c_{55} - c_{44} - 2ic_{45}) (1 + i\bar{\gamma}) \right] \frac{\partial \phi}{\partial \bar{\chi}} \right\} e^{i\theta} \\ & + \frac{1}{4} \left\{ \left[(c_{55} - c_{44} + 2ic_{45}) (1 - i\gamma) + (c_{55} + c_{44}) (1 + i\gamma) \right] \frac{\partial \phi}{\partial \chi} \right. \\ & \left. + \left[(c_{55} - c_{44} + 2ic_{45}) (1 - i\bar{\gamma}) + (c_{55} + c_{44}) (1 + i\bar{\gamma}) \right] \frac{\partial \phi}{\partial \bar{\chi}} \right\} e^{-i\theta}, \end{aligned} \tag{22}$$

$$\begin{aligned} \tau_{\theta z} = & \frac{1}{4} \left\{ \left[i \left(c_{44} + c_{55} \right) (1 - i\gamma) + \left(2c_{45} + i \left(c_{55} - c_{44} \right) \right) (1 + i\gamma) \right] \frac{\partial \phi}{\partial \chi} \right. \\ & \left. + \left[i \left(c_{44} + c_{55} \right) (1 - i\bar{\gamma}) + \left(2c_{45} + i \left(c_{55} - c_{44} \right) \right) (1 + i\bar{\gamma}) \right] \frac{\partial \phi}{\partial \bar{\chi}} \right\} e^{i\theta} \\ & + \frac{1}{4} \left\{ \left[\left(2c_{45} + i \left(c_{44} - c_{55} \right) \right) (1 - i\gamma) + i \left(c_{44} + c_{55} \right) (1 + i\gamma) \right] \frac{\partial \phi}{\partial \chi} \right. \\ & \left. + \left[\left(2c_{45} + i \left(c_{44} - c_{55} \right) \right) (1 - i\bar{\gamma}) - i \left(c_{44} + c_{55} \right) (1 + i\bar{\gamma}) \right] \frac{\partial \phi}{\partial \bar{\chi}} \right\} e^{-i\theta}. \end{aligned} \tag{23}$$

Substituting the wave fields into Eqs. (18)–(23), respectively, the specific expression of stress components can be obtained.

4 Boundary conditions

Considering the continuity condition at the boundary of the cylindrical inclusion, the boundary condition is the continuity condition of the displacement and radial shear stress, which can be written as

$$\phi_I = \phi_{II}, \quad |z| = R, \tag{24}$$

$$\tau_{rz,I} = \tau_{rz,II} \quad |z| = R. \tag{25}$$

Substituting the incident wave, reflected wave, scattering wave, and the standing wave into Eq. (24), and substituting the stress components into Eq. (25) at the same time, the boundary condition becomes

$$\sum_{n=-\infty}^{\infty} (A_n \xi_n - B_n \zeta_n) = \xi, \tag{26}$$

$$\sum_{n=-\infty}^{\infty} (A_n \varepsilon_n - B_n \eta_n) = \varepsilon \tag{27}$$

where

$$\xi_n = F_n + F_n', \tag{28}$$

$$\zeta_n = G_n, \tag{29}$$

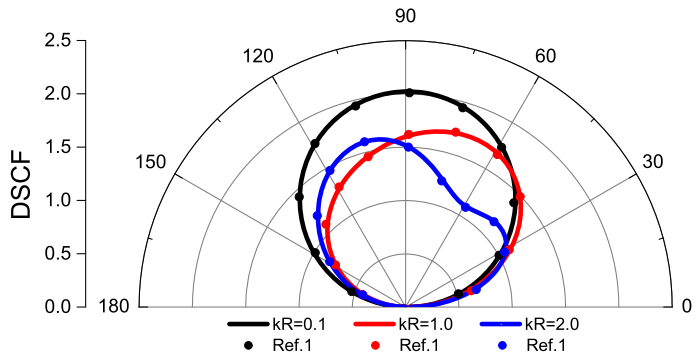

Fig. 2 Verification of DSCF by the degeneration procedure

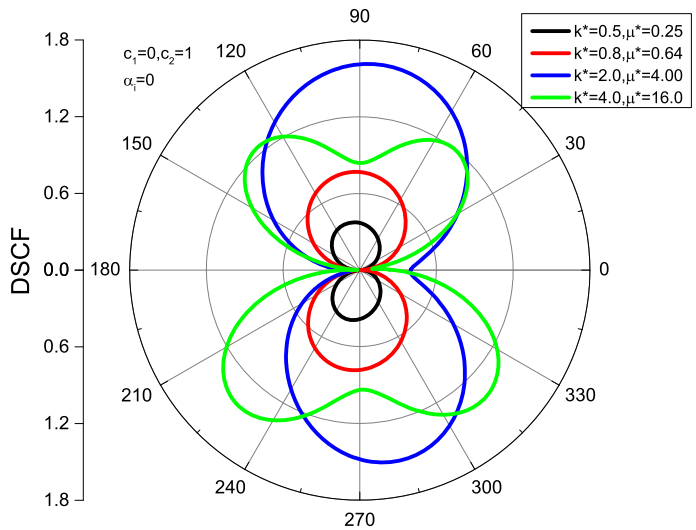

Fig. 3 Distribution of DSCF with $h/R = 2, kR = 1$

$$\xi = -\phi^{(i)} - \phi^{(r)}, \tag{30}$$

$$\varepsilon_n = k_T \left[(a+ic)\left(F_{n-1} - F'_{n-1}\right) - (b-ic)\left(F_{n+1} - F'_{n+1}\right)\right] e^{i\theta} + k_T \left[(b+ic)\left(F_{n-1} - F'_{n-1}\right) - (a-ic)\left(F_{n+1} - F'_{n+1}\right)\right] e^{-i\theta}, \tag{31}$$

$$\eta_n = 2k_2\mu_2 \left(G_{n-1}e^{i\theta} - G_{n+1}e^{-i\theta}\right), \tag{32}$$

$$\begin{aligned}\varepsilon = & -ik_i\phi^{(i)} \left\{\left[(c_{44}+c_{55})\beta_i + (c_{55}-c_{44}-2ic_{45})\bar{\beta}_i\right] e^{i\theta} \right. \\ & \left. + \left[(c_{55}-c_{44}+2ic_{45})\beta_i + (c_{44}+c_{55})\bar{\beta}_i\right] e^{-i\theta}\right\} \\ & -ik_r\phi^{(r)} \left\{\left[(c_{44}+c_{55})\beta_r + (c_{55}-c_{44}-2ic_{45})\bar{\beta}_r\right] e^{i\theta} \right. \\ & \left. + \left[(c_{55}-c_{44}+2ic_{45})\beta_r + (c_{44}+c_{55})\bar{\beta}_r\right] e^{-i\theta}\right\}. \end{aligned} \tag{33}$$

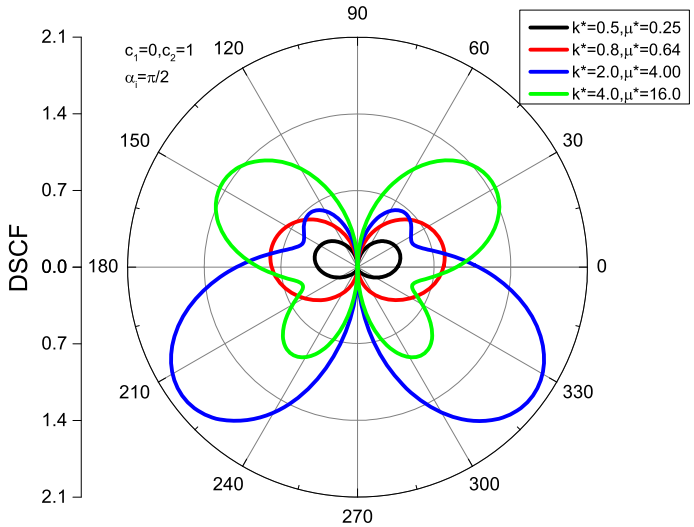

Fig. 4 Distribution of DSCF with $h/R = 2, kR = 1$

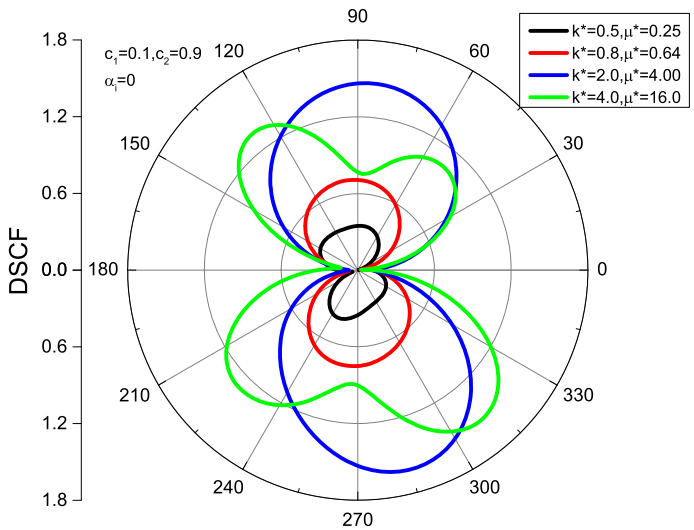

Fig. 5 Distribution of DSCF with $h/R = 2, kR = 1$

The expressions of F_n, F_n', G_n and the forms of a, b, and c in Eqs. (28)–(33) can be shown to be

$$F_n = H_n^{(1)}\left(k_T\left|\chi\right|\right)\left(\frac{\chi}{|\chi|}\right)^n, \tag{34}$$

$$F_n' = H_n^{(1)}\left(k_T\left|\chi_1\right|\right)\left(\frac{\chi_1}{|\chi_1|}\right)^{-n}, \tag{35}$$

$$G_n = J_n\left(k_2\left|z\right|\right)\left(\frac{z}{|z|}\right)^n, \tag{36}$$

$$a = \left(c_{55}c_{44} - c_{45}^2\right)^{\frac{1}{2}}\left[1 + \frac{\left(c_{55}c_{44} - c_{45}^2\right)^{\frac{1}{2}}}{c_{44}}\right], \tag{37}$$

$$b = -\left(c_{55}c_{44} - c_{45}^2\right)^{\frac{1}{2}}\left[1 - \frac{\left(c_{55}c_{44} - c_{45}^2\right)^{\frac{1}{2}}}{c_{44}}\right], \tag{38}$$

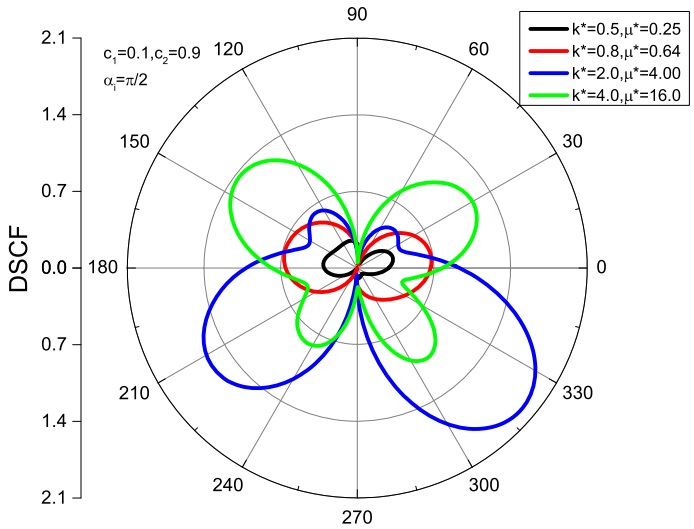

Fig. 6 Distribution of DSCF with $h/R = 2$, $kR = 1$

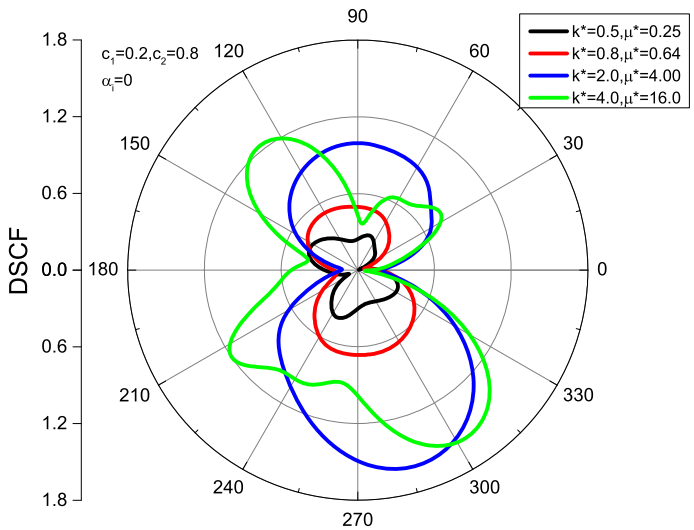

Fig. 7 Distribution of DSCF with $h/R = 2$, $kR = 1$

$$c = \frac{c_{45}\left(c_{55}c_{44} - c_{45}^2\right)^{\frac{1}{2}}}{c_{44}}. \tag{39}$$

Multiplying $e^{-im\theta}$ with both sides of Eqs. (26) and (27) and integrating on the interval $(-\pi, \pi)$ in order to solve the undefined coefficients A_n and B_n, one obtains

$$\sum_{n=-\infty}^{\infty} (A_n\xi_{mn} - B_n\zeta_{mn}) = \xi_m, \quad m = n = 0, \pm1, \pm2, \ldots \tag{40}$$

$$\sum_{n=-\infty}^{\infty} (A_n\varepsilon_{mn} - B_n\eta_{mn}) = \varepsilon_m, \quad m = n = 0, \pm1, \pm2, \ldots \tag{41}$$

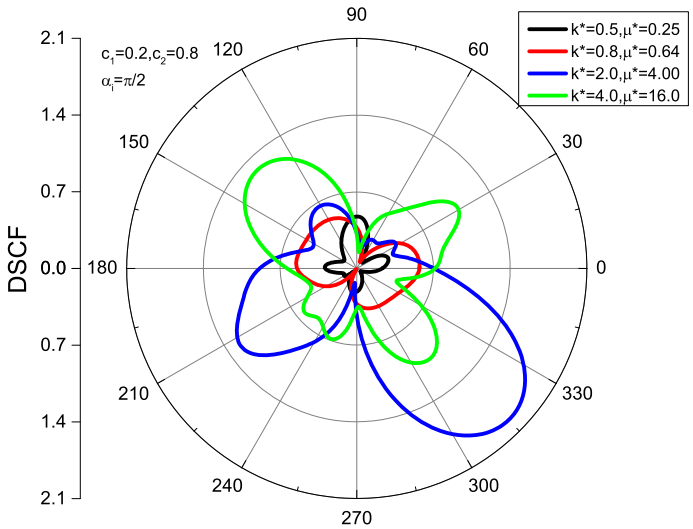

Fig. 8 Distribution of DSCF with $h/R = 2, kR = 1$

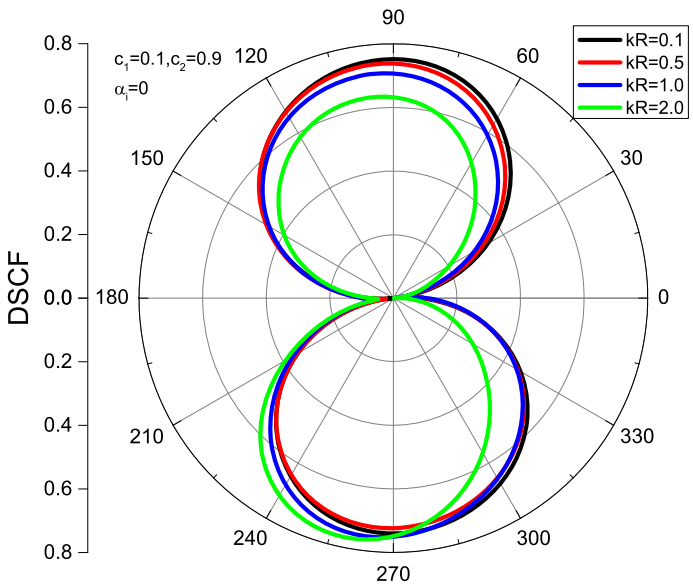

Fig. 9 Distribution of DSCF with $h/R = 2, k^* = 0.8$

where

$$\xi_{mn} = \frac{1}{2\pi}\int_{-\pi}^{\pi} \xi_n e^{-im\theta}\mathrm{d}\theta,\ \zeta_{mn} = \frac{1}{2\pi}\int_{-\pi}^{\pi} \zeta_n e^{-im\theta}\mathrm{d}\theta,\ \xi_m = \frac{1}{2\pi}\int_{-\pi}^{\pi} \xi e^{-im\theta}d\theta, \tag{42}$$

$$\varepsilon_{mn} = \frac{1}{2\pi}\int_{-\pi}^{\pi} \varepsilon_n e^{-im\theta}\mathrm{d}\theta,\ \eta_{mn} = \frac{1}{2\pi}\int_{-\pi}^{\pi} \eta_n e^{-im\theta}\mathrm{d}\theta,\ \varepsilon_m = \frac{1}{2\pi}\int_{-\pi}^{\pi} \varepsilon e^{-im\theta}d\theta. \tag{43}$$

5 Dynamic stress concentration factor (DSCF)

According to the definition of the dynamic stress concentration factor, the DSCF is the ratio of the hoop stress to the stress τ_0 (induced by the incident wave), which has the form

$$\tau^*_{\theta z} = |\tau_{\theta z}/\tau_0\ | \tag{44}$$

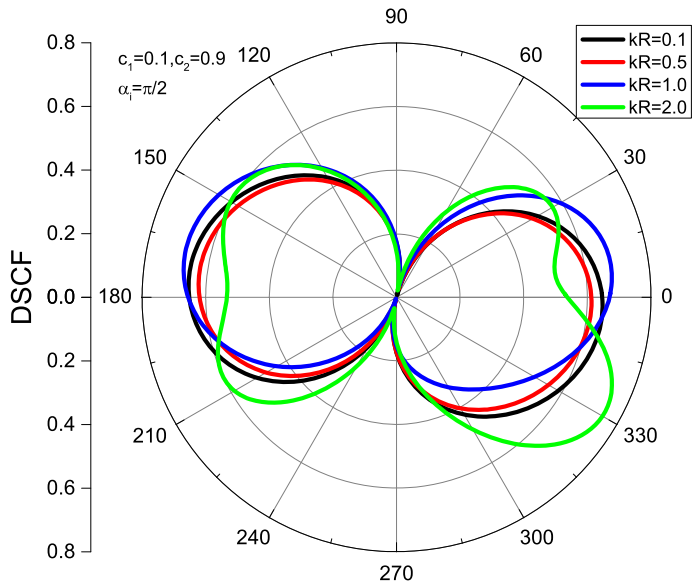

Fig. 10 Distribution of DSCF with $h/R = 2, k^* = 0.8$

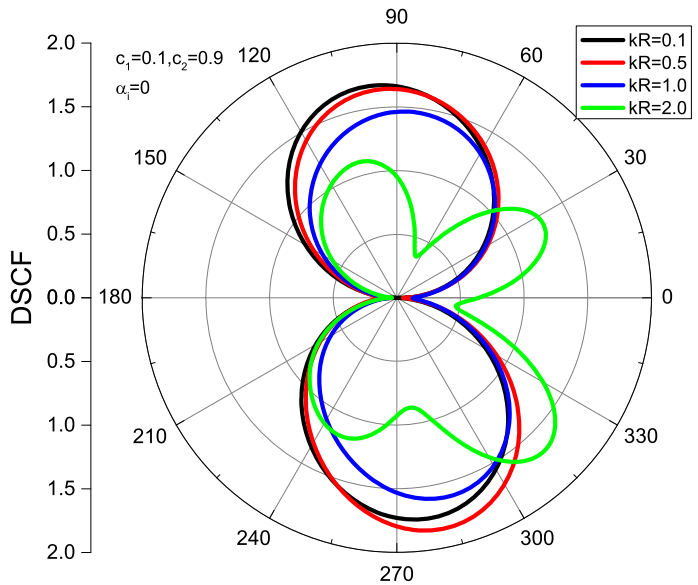

Fig. 11 Distribution of DSCF with $h/R = 2, k^* = 0.8$

where $\tau_0 = c_{55}k_i\phi_0$. Substituting the wave fields into Eqs. (21) and (23), the hoop stress obeys

$$\begin{aligned}\tau_{\theta z} =& \frac{k_T}{4}\sum_{n=-\infty}^{\infty} A_n\left[\left(a'+ib'\right)\left(F_{n-1}-F'_{n+1}\right)-\left(-a'+ic'\right)\left(F_{n+1}-F'_{n-1}\right)\right]e^{i\theta}\\ &+\frac{k_T}{4}\sum_{n=-\infty}^{\infty} A_n\left[\left(-a'-ic'\right)\left(F_{n-1}-F'_{n+1}\right)-\left(a'-ib'\right)\left(F_{n+1}-F'_{n-1}\right)\right]e^{-i\theta}\\ &+\frac{ik_i\phi^{(i)}}{4}\left[i\left(c_{44}+c_{55}\right)\beta_i+\left(2c_{45}+ic_{55}-ic_{44}\right)\bar{\beta}_i\right]e^{i\theta}\\ &+\frac{ik_i\phi^{(i)}}{4}\left[\left(2c_{45}-ic_{55}+ic_{44}\right)\beta_i-i\left(c_{44}+c_{55}\right)\bar{\beta}_i\right]e^{-i\theta}\end{aligned}$$

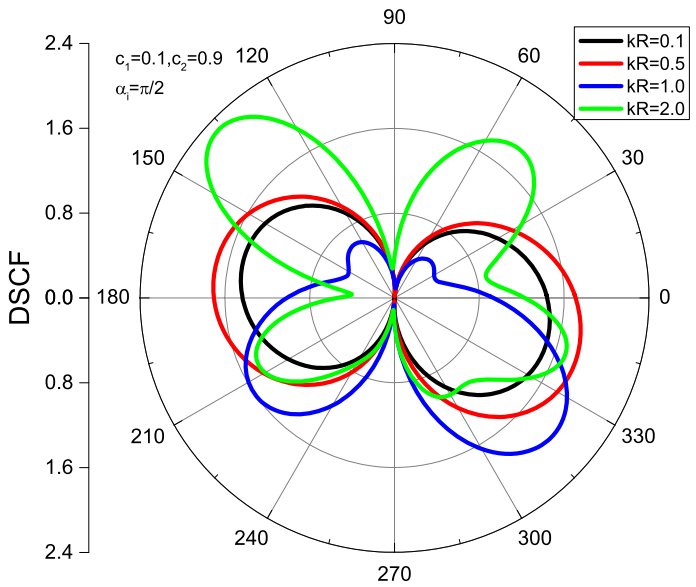

Fig. 12 Distribution of DSCF with $h/R = 2, k^* = 0.8$

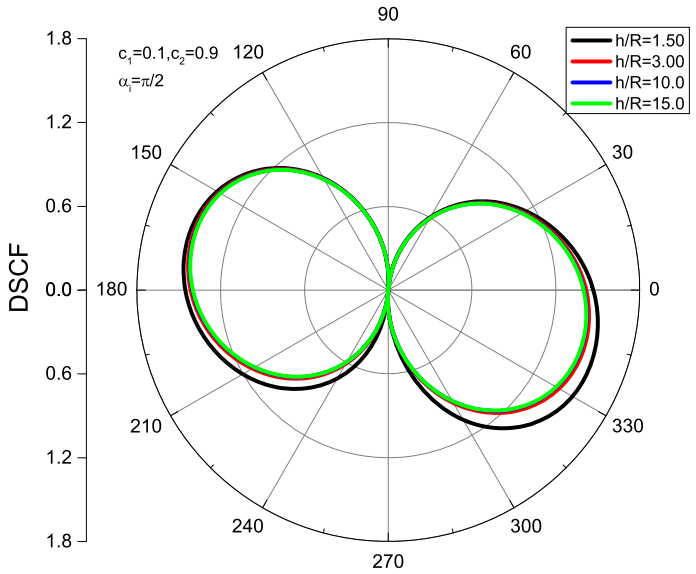

Fig. 13 Distribution of DSCF with $kR = 0.1, k^* = 2$

$$+\frac{ik_r\phi^{(r)}}{4}\left[i\left(c_{44}+c_{55}\right)\beta_r+\left(2c_{45}+ic_{55}-ic_{44}\right)\bar{\beta}_r\right]e^{i\theta}$$
$$+\frac{ik_r\phi^{(r)}}{4}\left[\left(2c_{45}-ic_{55}+ic_{44}\right)\beta_i-i\left(c_{44}+c_{55}\right)\bar{\beta}_r\right]e^{-i\theta} \quad (45)$$

where $a'=-c, b'=a, c'=b$.

6 Numerical results and solution analysis

In order to verify the validity of the method presented in this paper, we set $\mu_2=0$ to degenerate the inclusion into a cavity. Meanwhile, the depth of the inclusion is modified into fifty, and the anisotropic parameter is set as $c_{44}=1, c_{45}=0, c_{55}=1$ to contrast with the solution obtained by Pao et al. (in Ref. 1) in Fig. 2. Figure 2 shows that the degenerate results are coincident with the solution calculated by Pao et al. perfectly.

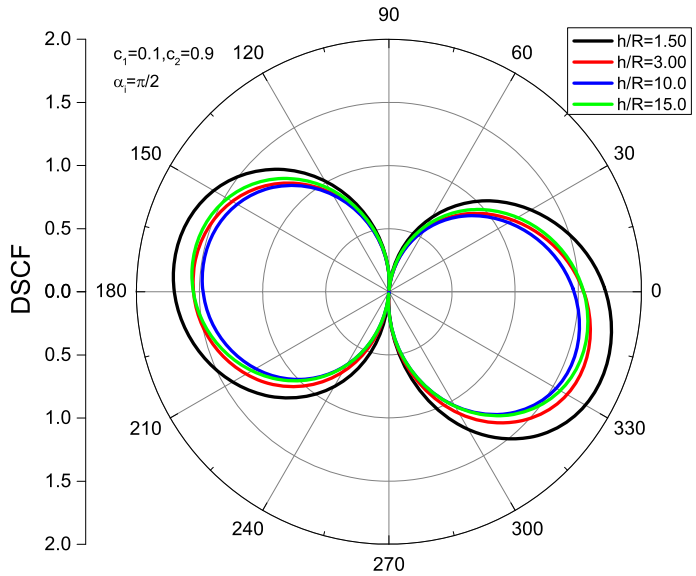

Fig. 14 Distribution of DSCF with $kR=0.5, k^*=2$

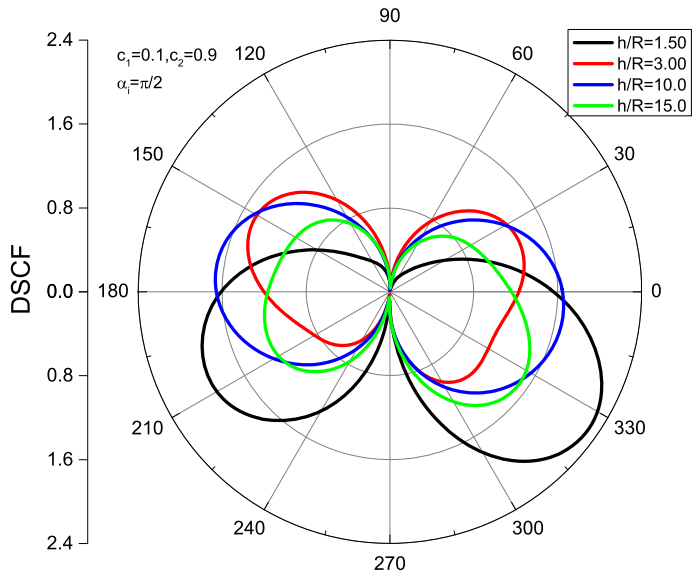

Fig. 15 Distribution of DSCF with $kR=1.0, k^*=2$

The distribution of the DSCF around the inclusion is presented in Figs. 3, 4, 5, 6, 7, and 8 for different anisotropic parameters. With the purpose of showing the anisotropy in different directions, two new parameters $c_1 = c_{45}/c_{55}$ and $c_2 = c_{44}/c_{55}$ are introduced. Moreover, wave numbers ratio $k^* = k_2/k_1$ and shear modulus ratio $\mu^* = \mu_1/\mu_2$ are defined to show the property relation between the inclusion and the half space. It can be inferred that $\mu^* > 1$ ($k^* > 1$) represents that the medium I is harder than the medium II while $\mu^* < 1$ ($k^* < 1$) signifies the opposite condition.

Figures 3 and 4 show the distribution of DSCF with different k^* and μ^* when the incident wave angle is $\alpha_i = 0$ and $\pi/2$. The dimensionless incident wave number is kR and $kR = 1$, the depth of the inclusion is $h/R = 2$. $c_1 = 0$ and $c_2 = 1$ represent the medium I which is homogeneous and isotropic. If the inclusion is softer than the half space, the dynamic stress concentration factor becomes larger. That means the soft inclusion embedded in the half space will enhance the stresses around it. Moreover, the distribution of DSCF becomes complex with the k^* augments. In Fig. 4, the DSCF displays a symmetric distribution along the y-axis because the background medium (medium I) is isotropic, and the incident angle is $\pi/2$.

Figures 5, 6, 7, and 8 demonstrate the distribution of the DSCF around the inclusion when the half space is anisotropic. The dynamic stress concentration factor is still larger when the inclusion is softer than the half space. However, because the background is anisotropic, the DSCF does not have a symmetric distribution anymore, and the distribution of the DSCF turns more complex at the same time. Then, in contrast with the case when the half space is isotropic, the distribution of the DSCF seems distorted. When $k^* = 0.5$, 2.0, 4.0, the DSCF distorts evidently, but it changes little when $k^* = 0.8$, that is because the properties of internal and external medium are similar. The maximum of the DSCF varies little when the half space is anisotropic. It approximately equals 1.5 when $\alpha_i = 0$ and 2.1 when $\alpha_i = \pi/2$.

The distribution of the DSCF with different dimensionless incident wave numbers is shown in Figs. 9, 10, 11, and 12. The incident wave angle is $\alpha_i = 0$ and $\alpha_i = \pi/2$, and the background medium is anisotropic. Two cases are considered ($k^* = 0.8$ and $k^* = 2$) in Figs. 9, 10, 11, and 12. With the increasing of the incident wave number, the DSCF distribution becomes complex. Besides, if the inclusion is harder than the half space, the maximum of the DSCF changes little with the incident wave number increasing, but if the inclusion is softer, the maximum of the DSCF varies apparently. This phenomenon indicates that the stresses around soft defects are significantly affected by the incident wave number.

Figures 13, 14, 15, and 16 present the distribution of the DSCF when the depth of inclusion h/R is 1.5, 3, 10, and 15. The background medium is anisotropic, and the wave numbers ratio is $k^* = 2$. When the incident wave number is small ($kR = 0.1$ and 0.5), the distribution of DSCF is nearly unchanged with the increase of h/R . However, when the incident wave number is large ($kR = 1$ and 2), the DSCF changes evidently with the h/R augments. The reason is when kR is small, the condition is the near static case, but when kR becomes large, the dynamic effects become clear. Furthermore, the values of the DSCF decrease when the depth of the

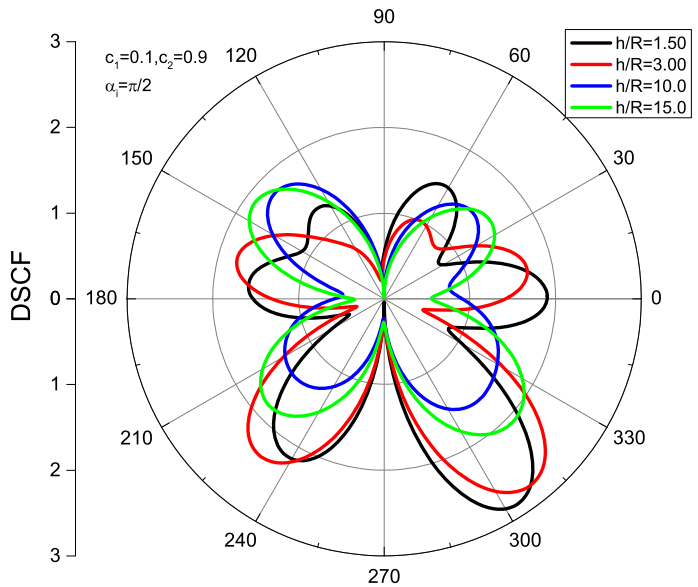

Fig. 16 Distribution of DSCF with $kR = 2.0$, $k^* = 2$

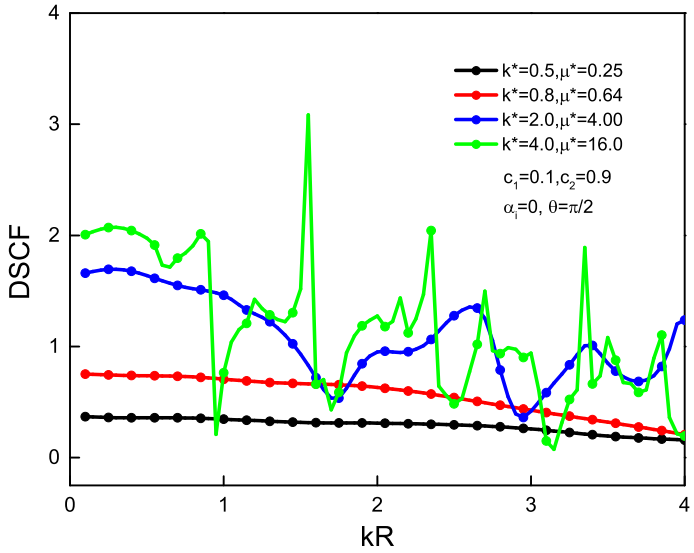

Fig. 17 Variation of DSCF with changing kR ($h/R = 2$)

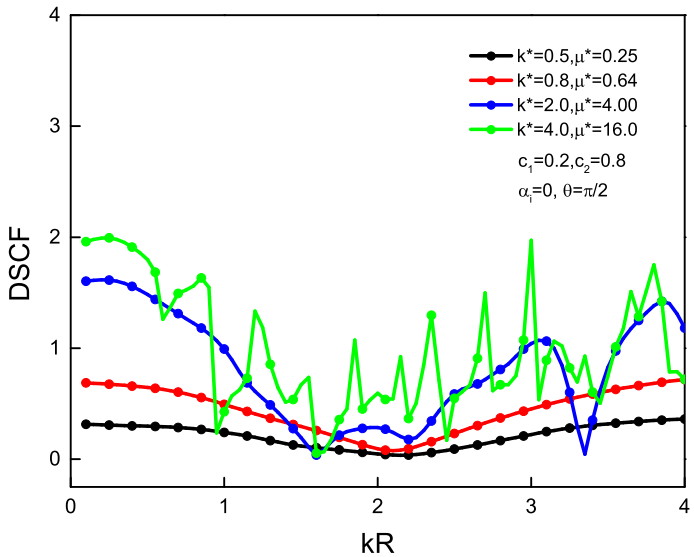

Fig. 18 Variation of DSCF with changing kR ($h/R = 2$)

inclusion grows, because the interplay between shallow burial inclusion and the surface is more intense than in case of the deep one. As the condition of deep burial inclusion the influences of the reflected wave on the inclusion turn small, and it can be regarded as infinite medium condition.

Figures 17 and 18 display the variation of the DSCF with changing incident wave number kR when the inclusion and the half space have different wave numbers ratio and shear modulus ratio. The burial depth of the inclusion is $h/R = 2$, and the point is $\theta = \pi/2$. Considering the case of hard inclusion ($k^* < 1$), the DSCFs at the inclusion are small, but the DSCFs become large when the inclusion is softer than the half space. This result is the same as we obtained in Figs. 3, 4, 5, 6, 7, and 8. Then, if the inclusion is softer than the half space, the DSCFs fluctuate obviously with the variation of the incident wave number. The phenomenon proves that the stresses around soft defects are significantly affected by the incident wave number again.

7 Conclusions

Based on the complex function method and multipolar coordinate system, the dynamic response of shear waves by a cylindrical inclusion is investigated. The governing equation is converted into its normal form, and the expressions of incident wave, reflected wave, scattering wave, and standing wave are obtained. According to the continuity condition at the boundary of the cylindrical inclusion, the unknown coefficients in the scattering wave and standing wave are found. Then, the dynamic stress concentration factor (DSCF) around the inclusion is calculated. The results reveal that the soft inclusion embedded in the half space will enhance the stresses around it, and the DSCF around the soft inclusion is influenced by the incident wave number evidently. This indicates that a soft inclusion in the medium can influence the mechanical properties around it significantly. So the dynamic problems of a medium with soft defects should be paid more attention in practical engineering. Then, with the increase of the incident wave number, the distribution of the DSCF becomes complex, which means high-frequency excitation may cause complicated structural damage. Moreover, the depth of the inclusion affects the distribution of the DSCF significantly when the incident wave number is large. So, an appropriate depth of the underground structure needs to be considered in practical engineering.

Acknowledgements This work was supported by the Scientific Research Fund of Institute of Engineering Mechanics, China Earthquake Administration (Grant No. 2017QJGJ06), the National Science and Technology Pillar Program (Grant No. 2015BAK17B06), the Earthquake Industry Special Science Research Foundation Project (Grant No. 201508026-02), the Fundamental Research Funds for the Central Universities (Grant No. HEUCF170202), and the Program for Innovative Research Team in China Earthquake Administration.

References

1. Pao, Y.H., Mow, C.C.: Diffraction of elastic waves and dynamic stress concentrations, pp. 114–304. Crane and Russak, New York (1973)
2. Achenbach, J.D.: Wave propagation in elastic solids. North-Holland Publishing Company, Amsterdam (1973)
3. Liu, D.K., Gai, B.Z., Tao, G.Y.: Applications of the method of complex functions to dynamic stress concentrations. Wave Motion **4**, 293–304 (1982)
4. Trifunac, M.D.: Scattering of plane SH waves by a semi-cylindrical canyon. Earthq. Eng. Struct. Dyn. **1**, 267–281 (1973)
5. Trifunac, M.D.: Scattering of plane SH waves by a semi-elliptical canyon. Earthq. Eng. Struct. Dyn. **3**, 157–169 (1974)
6. Parvanova, S.L., Dineva, P.S., Manolis, G.D., Kochev, P.N.: Dynamic response of a solid with multiple inclusions under anti-plane strain conditions by the BEM. Comput. Struct. **139**, 65–83 (2014)
7. Sheikhhassani, R., Dravinski, M.: Dynamic stress concentration for multiple multilayered inclusions embedded in an elastic half-space subjected to SH-waves. Wave Motion **62**, 20–40 (2016)
8. Xu, H.N., Yang, Z.L., Wang, S.S.: Dynamics response of complex defects near bimaterials interface by incident out-plane waves. Acta Mech. **227**, 1251–1264 (2016)
9. Eskandari, M., Samea, P., Ahmadi, S.F.: Axisymmetric time-harmonic response of a surface-stiffened transversely isotropic half-space. Meccanica **52**, 1–14 (2016)
10. Liu, D.K., Han, F.: The scattering of plane SH-waves by noncircular cavity in anisotropic media. J. Appl. Mech. **60**, 769–772 (1993)
11. Eslami, H., Gatmiri, B.: Two formulations for dynamic response of a cylindrical cavity in cross-anisotropic porous media. Int. J. Numer. Anal. Methods Geomech. **34**, 331–356 (2010)
12. Daros, C.H.: Greens function for SH-waves in inhomogeneous anisotropic elastic solid with power-function velocity variation. Wave Motion **50**, 101–110 (2013)
13. Baydoun, I., Savin, E., Cottereau, R., et al.: Kinetic modeling of multiple scattering of elastic waves in heterogeneous anisotropic media. Wave Motion **51**, 1325–1348 (2014)
14. Wang, X., Schiavone, P.: Surface and interfacial waves in anisotropic elastic quasicrystals. Wave Motion **51**, 77–85 (2014)
15. Djeran-Maigre, I., Kuznetsov, S.V.: Velocities, dispersion, and energy of SH-waves in anisotropic laminated plates. Acoust. Phys. **60**, 200–207 (2014)
16. Boström, A.: Scattering by an anisotropic circle. Wave Motion **57**, 239–244 (2015)
17. Li, J., Rokhlin, S.I.: Elastic wave scattering in random anisotropic solids. Int. J. Solids Struct. **78–79**, 110–124 (2016)
18. Lee, J., Lee, H., Jeong, H.: Numerical analysis of SH wave field calculations for various types of a multilayered anisotropic inclusion. Eng. Anal. Bound. Elem. **64**, 38–67 (2016)
19. Liu, D.K., Han, F.: Scattering of plane SH-wave by canyon topography in anisotropic medium. Earthq. Eng. Eng. Vib. **10**, 11–25 (1990). (**in Chinese**)